miR-130a expression is related to aortic dilation in bicuspid aortic valve children

Borja Antequera González† (1, 2), Rosa Collell Hernández† (3), Neus Martínez Micaelo (1), Cristina Marimon Blanch (3), Bàrbara Carbonell (1, 2), Joaquín Escribano (3), Josep M. Alegret * (1, 2)

1. Group of Cardiovascular Research, Pere Virgili Health Research Institute (IISPV), Universitat Rovira i Virgili, 43204 Reus, Spain

2) Cardiology Department, Hospital Universitari Sant Joan de Reus, Universitat Rovira i Virgili, 43204 Reus, Spain

3) Pediatric Department, Hospital Universitari Sant Joan de Reus, Universitat Rovira i Virgili, 43204 Reus, Spain

† These authors contributed equally to this study.

* Corresponding author:

Josep M. Alegret

Avinguda del Doctor Josep Laporte, 2

Cardiology Department

Reus, TG 43204

Spain

txalegret@hotmail.com; 977310300, Ext. 50087.

Impact:

- miR-130a expression in plasma is related to aortic dilation in bicuspid aortic valve (BAV) children.
- To our knowledge, this is the first study that analyses miRNA patterns in bicuspid aortic valve children with aortic dilation.
- miR-130a expression in plasma could be a biomarker in order to help differentiate low-to high-risk BAV children, which is vitally important for advanced care planning.

Abstract:

Purpose: Bicuspid aortic valve disease (BAV) is present in 0.5-2% of the population and can promote aortic dilation, eventually leading to fatal consequences. Although some biomarkers have been proposed in adults, no studies have tested these candidates in children. We aimed to evaluate 4 miRNAs previously described to be related to BAV disease and aortic dilation in adults in a pediatric cohort. Methods: Eighty participants ≤ 17 years old (4-17; mean 12) were included. From the BAV group, 40% had a dilated aorta (z score>2). RT–qPCR were performed in plasma samples to quantify miR-122, miR-130a, miR-486, and miR-718 using the delta-delta Ct method. Functional and enrichment analyses of miR-130a were also performed. Results: miR-130a expression in plasma was found to be significantly lower in BAV patients with a dilated aorta verses nondilated patients (p= 0.008) and healthy TAV controls (p= 0.004). Furthermore, miR-130a expression in plasma was inversely correlated with ascending aorta (r=0.318, p=0.004) and aortic root z scores (r=0.322; p=0.004). Enrichment analysis showed that miR-130a target genes are related to the TGFß signalling pathway. Conclusions: miR-130a expression in plasma is decreased in aortic dilated BAV children compared to nondilated BAV children , helping differentiate low- to high-risk patients.

Introduction:

Bicuspid aortic valve (BAV) disease is present in 0.5-2% of the general population and is defined by the abnormal morphology of the valve, composed of two cusps instead of three, usually by the fusion of two of them[1–3]. This morphological anomaly can lead to valve dysfunction (aortic insufficiency, aortic stenosis) and is related to a high prevalence of ascending aorta dilation[4,5]. Specifically, aortic dilation is present in more than 50% of the BAV population, and its progression can lead to fatal consequences, including aortic aneurysm and dissection[6,7]. Although the mechanisms that underlie aortic dilation are not clear, haemodynamic alterations and genetic abnormalities in BAV disease have been proposed for the defective structure of the aorta[8,9]. Additionally, some studies have suggested that oxidative stress and consequently endothelial dysfunction are present in BAV disease[10–12].

BAV disease in children is usually asymptomatic, although it has been estimated that 1 of 50 adolescents have clinically significant valve disease[13,14]. Aortic dilation has been previously described by many clinicians to have correlations with children, indicating that the progression of aortic dilation may develop at younger ages[15–17]. Although the risk of aneurysm progression in pediatric patients is scarce, identifying children with BAV disease and aortic dilation is vitally important for advanced care planning.

Currently, there are no definite established biomarkers for BAV disease and aortic dilation that help differentiate high- to low-risk patients. While some studies have linked aortic dilation to different microRNA (miRNA) patterns in BAV adults, none of them have studied its possible potential in children[18–22]. The use of miRNAs for biomarker purposes has been widely extended in the last few years, and miRNAs are currently used in many cardiovascular diseases[23]. miRNAs are RNA molecules of 18-24 nucleotides that are capable of modifying gene expression at the posttranscriptional level by binding to messenger RNA (mRNA)[24]. miRNAs are highly expressed in blood, as well as every cell, and their expression pattern can be specific for different pathologies, making them perfect candidates for biomarker purposes[25]. Our group has previously presented a miRNA pattern present in BAV patients with aortic dilation in an adult cohort. Hence, in this study, we aimed to evaluate the potential of these 4 miRNA candidates (miR-122, miR-130a, miR-486, and miR-718) as biomarkers of aortic valve morphology as well as aortic dilation in the pediatric population.

Material & methods:

Study population:

This study included a cohort of 80 patients aged ≤ 17 years old (4-17) who were prospectively included and followed-up in our facilities. Half of them, 40, corresponded to consecutive children diagnosed with BAV disease. The other half of them corresponded to a group of 40 healthy TAV controls adjusted by age and sex recruited during follow-ups in sports medicine. The diagnosis of BAV disease was made when two aortic leaflets were clearly visualized, with or without a raphe, on the parasternal short-axis view of a transthoracic echocardiogram. A dilated aortic root or ascending aorta was diagnosed when the aortic diameter was measured in diastole using the leading edge technique, with a z score>2 for the Paris reference source[26]. Patients with an aortic root or ascending aorta z score >2 were classified as dilated (BAV_DIL), whereas the other patients were considered nondilated (BAV_nonDIL). All explorations were performed or supervised by the same observer. Upon enrollment, participants were prospectively entered into a specific database, underwent a blood draw and provided informed written consent. Samples were stored until needed in our biological sample bank (Biobanc IISPV-HUSJR).

Blood sampling:

Blood samples were collected in overnight fasting conditions and were processed within 90 mins after collection. The samples were centrifuged at 1500 × g for 15 min to obtain plasma. The plasma samples were stored at −80 °C in our biological sample bank until needed (Biobanc IISPV-HUSJR).

RNA extraction:

RNA was extracted and purified from 200 µL of plasma using the miRNeasy serum/plasma advanced kit following the manufacturer's instructions (#217204, Qiagen). To increase RNA recovery, 1 µg of MS2 carrier RNA was added to each plasma sample (#10165948001, Roche). RNA quantity and quality (A260/A280) was checked before its use for RT-qPCR with Biotek Microplate Reader Synergy HT.

miRNA quantification by RT–qPCR:

RNA obtained from the plasma samples was used for cDNA synthesis with TaqMan™ Advanced (Applied Biosystems, #A28007) according to the manufacturer's protocol in four steps (poly-A tailing, adaptor ligation, reverse transcription and miR amplification). miRNA levels were quantified with qPCR. TaqMan™ Fast Advanced Master Mix kit (Applied Biosystems, #4444963) with TaqMan™ Advanced probes were used for quantification of miR-122 (477855_mir), miR-130a (477851_mir), and miR-486 (478128_mir) using LightCycler96 (Roche) under the following conditions: enzyme activation 20 s and amplification for 40 cycles (95º C 3 s for denature and 60 º C 30s for annealing). For mi-R718 quantification, the miRCURY LNA RT Kit (Qiagen, #339340) was used for reverse transcription following manufacturer's protocol (42º C 60 min, 95º C 5 min) and the miRCURY LNA SYBR Green PCR Kit (Qiagen, #339346) and hsa-miR-718 miRCURY LNA miRNA PCR Assay (Qiagen, #YP00205702) were used for qPCR under the following conditions: PCR initial heat activation (2 min, 95 °C); 2-step cycling for 40 cycles (denaturation 95º C 10 s and combines annealing/extension for 56º C 60 s). All reactions were performed in duplicates. In both qPCR kits, miR-16 was also measured (477860_mir for TaqMan™ Advanced Probes and #YP02119603 for Qiagen). miRNA expression levels were calculated using $2^{-\Delta\Delta Ct}$ method based on the relative expression of miR-16. miRNA levels are represented with ΔCt in this manuscript, including tables and figures.

Functional and pathway enrichment analysis of miR-130a

Target genes of miR-130a were predicted using the latest version available of miRwalk (http://mirwalk.umm.uni-heidelberg.de, v. Jan22)[27]. For clear visualization and representation of these target genes, miRTargetLink v.2.0 (https://ccb-compute.cs.uni-saarland.de/mirtargetlink2) was used[28]. After obtaining and representing the target genes of miR-130a, the Enrich database[29,30] (http://amp.pharm.mssm.edu/Enrichr/) was utilized to explore pathway analysis (Reactome 2022 database) and disease association study (DisGeNET database). The representation of these results was performed using Prism v9 (GraphPad Software, La Jolla, CA, USA).

Statistical analysis:

Statistical studies were performed to compare the distribution of the different variables between different groups. Categorical variables are expressed as percentages, and significant differences were identified using the chi-square test or Fisher's exact test, as appropriate. The quantitative variables, represented as the mean standard deviation (SD), were analysed using Student's t test. Pearson's or Spearman correlation, depending on the distribution (Shapiro-Wilk test), was used to identify the linear relationships between variables. One-way ANOVA was performed when comparing more than 2 groups, and Tukey's test was used for individual comparisons. Furthermore, a logistic regression with a forward stepwise model was constructed, and parameters with the strongest correlations to the dependent variable were included. Linear forward regression was also performed. In both multivariate analyses, a forward stepwise method was performed, which helped reduce the number of significant parameters that were selected in the final model. Differences were considered statistically significant when $p < 0.05$ (marked with asterisks, *$p < 0.05$; **$p < 0.005$; ***$p<0.001$; ****$p<0.0001$). For every graph and table, the mean value and standard deviation were represented. AUC analysis was also performed to evaluate the quality of the model and prediction of aortic dilation. All analyses were performed using SPSS v25 (IBM Corp., Armonk, NY, USA), and graphs were designed using Prism v9 (GraphPad Software, La Jolla, CA, USA).

Results:

Clinical and echocardiographic characteristics of the cohort:

The complete cohort (n: 80) was divided into three groups: TAV (n: 40) vs. BAV without aortic dilation (BAV_nonDIL, n: 24) vs. BAV with aortic dilation (BAV_DIL, n: 16). Clinical and echocardiographic characteristic comparisons can be found in Table 1. We observed greater aortic diameters and aortic valve gradients, as well as a higher prevalence of aortic insufficiency, in both BAV groups when compared to the healthy TAV control group. These parameters were also higher in the BAV_DIL group than in the BAV_nonDIL group. Age, sex, and body surface area (BSA) were not significantly different between the groups.

miRNA pattern is related to aortic dilation in BAV children

After quantifying miR-122, miR-130a, miR-486, and miR-718 expression in plasma, the complete miRNA pattern was compared (Table 2 and Figure 1). We identified miR-130a as the only miRNA differentially expressed between the three groups (p=0.008). Individual comparisons also showed that miR-130a dCt was significantly increased when comparing TAV vs. BAV_DIL (p=0.004) and BAV_nonDIL vs. BAV_DIL (p=0.013), but no significant changes were found when comparing TAV vs. BAV_noDIL (p=0.326) between the three groups. The rest of the miRNAs measured (miR-122, miR-486, and miR-718) did not show any significant changes between groups in the child cohort.

Furthermore, an area under the curve (AUC) graph was generated with baseline clinical parameters (sex, age, and BSA) to analyse the power prediction of a set of parameters (Figure 2). Different curves were prepared by adding valve morphology and subsequently miR-130a dCt. The results showed that adding valve morphology increased the AUC from 0.63 to 0.75 (p 0.002), but it reached 0.90 when adding miR-130a dCt (p<0.001) (Table 3).

Subsequently, we evaluated the relationship between miR-130a and aortic diameter parameters. We performed a correlation study between aortic root and ascending aorta z scores and the miRNA pattern (Table 4). In this case, miR-130a dCt was the only miRNA related to both z scores in the complete cohort (TAV + BAV) and in BAV children (Figure 3).

A multivariate linear analysis was also performed for both aortic root and ascending aorta z scores to determine miR-130a dCt independency. The initial model included miR-130a dCt, sex, age and BSA. In both cases, only miR-130a dCt persisted as an independent predictor of the z score in children (Table 5).

Functional and pathway enrichment analysis of miR-130a:

To provide a better understanding of the relevance of miR-130a downregulation in aortic dilated BAV children, we characterized the putative biological functions of this miRNA based on the identification of the miR-130a target genes. The predicted miRNA-gene interaction network was composed of miR-130a (hsa-miR-130a-3p) and 250 target genes, but only the 32 strongest related genes were included in Figure 4 for better visualization.

A functional enrichment analysis was also performed to predict the associated signalling pathways and related diseases of the miR-130a target genes. Although numerous signalling pathways were predicted to be related to miR-130a expression, many of them are linked to the TGFß signalling pathway, oxidative stress, and extracellular vesicle metabolism. The top 10 miR-130a target gene-associated pathways are represented in Figure 5. In addition to cell signalling processes, an association between miR-130a target genes and related diseases was analysed and is represented in Figure 6. Cardiovascular diseases were the diseases most related to the miR-130a target genes.

DISCUSSION

In this study, we analysed the miRNA pattern in plasma in children with BAV disease and aortic dilation to confirm the previously found alterations that occur in adult patients. Although miRNA expression seemed to behave differently at younger ages, we found miR-130a to be highly related to aortic dilation in children, specifically in BAV children. miR-130a expression in plasma was significantly lower in dilated patients, and both ascending aorta and aortic root z scores were strongly correlated with miR-130a dCt.

BAV disease can significantly increase the possibility of diverse associated aortopathies, such as aortic dilation[4,31]. Aortic dilation is present in more than 50% of BAV patients, and it is known to progress faster in these patients. Furthermore, its latest stages can be fatal, concluding in aortic aneurysm and dissection[4,31]. Aortic dilation in BAV children can easily go unnoticed since it does not show clear symptoms until later stages. Therefore, it seems of special importance to have biomarkers that can help identify high-risk patients to increase the plan for a better follow-up strategy. In the last few years, miRNAs have been widely studied in different pathologies, mainly in adults, resulting in important discoveries of independent biomarkers for cardiovascular diseases, among others[23,32]. Furthermore, miRNA differential expression has also helped elucidate the pathophysiology and development of diverse cardiovascular diseases[32]. Unfortunately, in children, the number of studies is very small, and to date, we have not been able to find any studies regarding miRNA expression in a cohort of BAV children, which also adds value to our results.

Although it is not yet fully understood, the mechanisms that underlie aortic dilation include numerous and diverse genetic abnormalities, as well as haemodynamic alterations generated by the anomalous valve morphology[8,9,33]. These changes in blood flow can increase wall shear stress in the aorta and promote extracellular matrix dysregulation and elastic fibre degeneration, which may induce aortic dilation[34–36]. Furthermore, these blood flow alterations can also promote medial degeneration by metalloprotease pathways[37,38]. These factors could contribute to faulty aortic media in BAV patients. On the other hand, some studies suggest that endothelial dysfunction and oxidative stress could also play an important role in BAV disease, as well as in aortic dilation. Endothelial dysfunction has widely been discussed in BAV disease[12]. While some studies have focused on plasma biomarkers such as asymmetric dimethylarginine (ADMA)[39], others have focused their research on *in vitro* studies, showing impaired functionality of circulating endothelial cells in BAV disease[40]. Recent studies have also suggested that endothelial-to-mesenchymal transition, induced by TGFß, may be altered in BAV disease[41,42]. Our group has previously discussed poor antioxidant capacity in aortic dilated adult BAV patients, as well as higher expression of endothelial microparticles in plasma, a biomarker for endothelial dysfunction[18,43]. A specific miRNA pattern has also been proposed in BAV disease and aortic dilation in adults, which was also linked to TGFß signalling and endothelial damage[18,19].

We previously performed a discovery microarray to identify a differential miRNA pattern corresponding to BAV morphology and aortic dilation. In that study, four miRNAs were identified: miR-122, miR-130a, miR-486, and miR-718[18,19]. Therefore, we aimed to test whether this miRNA pattern was similarly expressed in BAV children with or without aortic dilation. Our previous results showed that in adults, miR-122, miR-130a and miR-486 were highly influenced by the aortic valve morphology whereas miR-718 was found to be an independent predictor of ascending aorta diameter. Nevertheless, this study has revealed that in a pediatric population, miR-130a emerged as an interesting biomarker candidate for aortic dilation in children, specifically in BAV children. miR-130a was inferiorly expressed in plasma in children with aortic dilation compared to nondilated children. Furthermore, miR-130a dCT showed strong correlations to aortic root and ascending aorta z score, both in the complete cohort, but above all, in the BAV children group. The rest of the miRNAs did not present significant differences between the analysed groups in pediatric ages, differing with the miRNA profile changes in an adult population.

Although the role of miR-130a needs further research, the enrichment analysis has helped us link miR-130a, aortic dilation and different processes, such as TGFß signalling, oxidative stress, or even extracellular vesicle transport. Our previous work has already discussed poor antioxidant capacity, endothelial damage, and TGFß imbalance in aortic dilation in BAV adults due to alterations in miRNA patterns [12,19,43,44]. Bibliography research has complemented these findings, since many studies in adults have already associated differential miR-130a expression with different cardiovascular diseases. It has been shown to have a cardioprotective role and can even help predict cardiovascular risk in some studies[45,46]. Furthermore, its decreased expression has been associated with endothelial cell senescence [47]. Other studies have also discussed its role in the regulation of the vascular pattern during embryogenesis [48] and have linked miR-130a to the attenuation of cardiac fibrosis through TGF-ß/SMAD signalling [49]. Finally, TGFß signalling has also been associated with endothelial-to-mesenchymal transition (endoMT), which has also been highlighted to be altered in the ascending aortas of BAV patients[41,42]. Combined, this data has helped us hypothesize that miR-130a expression may be related to alterations in diverse signalling processes, such as the TGFß signalling pathway, which could lead to endothelial dysfunction and endoMT alterations [12,44]. Hence, the endothelium homeostasis imbalance may alter the endothelial barrier in the aorta, leading to faster aortic dilation in these BAV children. Nevertheless, future studies focused on analysing functional alterations caused by miR-130a should be assessed to confirm this hypothesis.

Conclusions:

We propose miR-130a as a solid biomarker candidate for aortic dilation in a pediatric population with BAV. Enrichment analysis also showed that miR-130a expression is related to TGFß signalling alterations, which could lead to endothelial dysfunction, a mechanism involved in the pathogenesis of aortic dilation.

Data Availability Statement: The data presented in this study are available on request from the corresponding author. The data are not publicly available due to ethical reasons.

Limitations: although the sample size of this study was enough for obtaining significant results, these miRNAs alteration expressions should be validated in a larger cohort, as well as the utility of miR-130a a as biomarker for aortic dilation in BAV children. Furthermore, we cannot decide miR-130a expression

alteration is the cause or the consequence of aortic dilation in BAV children. A longitudinal study could be helpful in giving us more information about these aspects.

References:

1. Braverman, A. C. *et al.* The bicuspid aortic valve. *Curr Probl Cardiol* **30**, 470–522 (2005).
2. Hoffman, J. I. E. & Kaplan, S. The incidence of congenital heart disease. *J. Am. Coll. Cardiol.* **39**, 1890–1900 (2002).
3. Sun, B. J. *et al.* Performance of a Simplified Dichotomous Phenotypic Classification of Bicuspid Aortic Valve to Predict Type of Valvulopathy and Combined Aortopathy. *J Am Soc Echocardiogr* **30**, 1152–1161 (2017).
4. D, D. *et al.* Aortic dilatation patterns and rates in adults with bicuspid aortic valves: a comparative study with Marfan syndrome and degenerative aortopathy. *Heart (British Cardiac Society)* **100**, (2014).
5. Michelena, H. I. *et al.* Incidence of aortic complications in patients with bicuspid aortic valves. *JAMA* **306**, 1104–1112 (2011).
6. Michelena, H. I. *et al.* Natural history of asymptomatic patients with normally functioning or minimally dysfunctional bicuspid aortic valve in the community. *Circulation* **117**, 2776–2784 (2008).
7. Alegret, J. M., Palomares, R., Duran, I., Vernis, J. M. & Palazón, Ó. Effect of Age on Valvular Dysfunction and Aortic Dilatation in Patients With a Bicuspid Aortic Valve. *Rev Esp Cardiol* **59**, 503–506 (2006).
8. Fedak, P. W. M. *et al.* Clinical and pathophysiological implications of a bicuspid aortic valve. *Circulation* **106**, 900–904 (2002).
9. Guala, A. *et al.* Influence of Aortic Dilation on the Regional Aortic Stiffness of Bicuspid Aortic

Valve Assessed by 4-Dimensional Flow Cardiac Magnetic Resonance: Comparison With Marfan Syndrome and Degenerative Aortic Aneurysm. *JACC Cardiovasc Imaging* **12**, 1020–1029 (2019).
10. Billaud, M. *et al.* Elevated oxidative stress in the aortic media of patients with bicuspid aortic valve. *J Thorac Cardiovasc Surg* **154**, 1756–1762 (2017).
11. Poggio, P. *et al.* MiRNA profiling revealed enhanced susceptibility to oxidative stress of endothelial cells from bicuspid aortic valve. *Journal of Molecular and Cellular Cardiology* **131**, 146–154 (2019).
12. Antequera-González, B., Martínez-Micaelo, N. & Alegret, J. M. Bicuspid Aortic Valve and Endothelial Dysfunction: Current Evidence and Potential Therapeutic Targets. *Front. Physiol.* **11**, 1015 (2020).
13. Hirsch Alan, T. *et al.* ACC/AHA 2005 Practice Guidelines for the Management of Patients With Peripheral Arterial Disease (Lower Extremity, Renal, Mesenteric, and Abdominal Aortic). *Circulation* **113**, e463–e654 (2006).
14. Siu, S. C. & Silversides, C. K. Bicuspid aortic valve disease. *J. Am. Coll. Cardiol.* **55**, 2789–2800 (2010).
15. Beroukhim, R. S., Kruzick, T. L., Taylor, A. L., Gao, D. & Yetman, A. T. Progression of aortic dilation in children with a functionally normal bicuspid aortic valve. *Am J Cardiol* **98**, 828–830 (2006).
16. Gurvitz, M., Chang, R.-K., Drant, S. & Allada, V. Frequency of aortic root dilation in children with a bicuspid aortic valve. *The American Journal of Cardiology* **94**, 1337–1340 (2004).
17. Ciotti, G. R., Vlahos, A. P. & Silverman, N. H. Morphology and Function of the Bicuspid Aortic Valve With and Without Coarctation of the Aorta in the Young. *The American Journal of Cardiology* **98**, 1096–1102 (2006).
18. Martínez-Micaelo, N., Beltrán-Debón, R., Aragonés, G., Faiges, M. & Alegret, J. M. MicroRNAs Clustered within the 14q32 Locus Are Associated with Endothelial Damage and Microparticle Secretion in Bicuspid Aortic Valve Disease. *Front. Physiol.* **8**, (2017).
19. Martínez-Micaelo, N., Beltrán-Debón, R., Baiges, I., Faiges, M. & Alegret, J. M. Specific circulating microRNA signature of bicuspid aortic valve disease. *J Transl Med* **15**, (2017).
20. Zhang, R.-M. *et al.* Fibrillin-1-regulated miR-122 has a critical role in thoracic aortic aneurysm formation. *Cell Mol Life Sci* **79**, 314 (2022).
21. Zhang, H. *et al.* Construction of the circRNA-miRNA-mRNA Regulatory Network of an Abdominal Aortic Aneurysm to Explore Its Potential Pathogenesis. *Dis Markers* **2021**, 9916881 (2021).
22. Wu, J. *et al.* Progressive Aortic Dilation Is Regulated by miR-17-Associated miRNAs. *J Am Coll Cardiol* **67**, 2965–2977 (2016).
23. Barwari, T., Joshi, A. & Mayr, M. MicroRNAs in Cardiovascular Disease. *J Am Coll Cardiol* **68**, 2577–2584 (2016).
24. Wahid, F., Shehzad, A., Khan, T. & Kim, Y. Y. MicroRNAs: synthesis, mechanism, function, and recent clinical trials. *Biochim Biophys Acta* **1803**, 1231–1243 (2010).
25. Klimczak, D., Pączek, L., Jażdżewski, K. & Kuch, M. MicroRNAs: powerful regulators and potential diagnostic tools in cardiovascular disease. *Kardiol Pol* **73**, 1–6 (2015).
26. Gautier, M. *et al.* Nomograms for aortic root diameters in children using two-dimensional echocardiography. *Am J Cardiol* **105**, 888–894 (2010).
27. Sticht, C., Torre, C. D. L., Parveen, A. & Gretz, N. miRWalk: An online resource for prediction of microRNA binding sites. *PLOS ONE* **13**, e0206239 (2018).
28. Kern, F. *et al.* miRTargetLink 2.0—interactive miRNA target gene and target pathway networks. *Nucleic Acids Res* **49**, W409–W416 (2021).
29. Chen, E. Y. *et al.* Enrichr: interactive and collaborative HTML5 gene list enrichment analysis tool. *BMC Bioinformatics* **14**, 128 (2013).
30. Kuleshov, M. V. *et al.* Enrichr: a comprehensive gene set enrichment analysis web server 2016 update. *Nucleic Acids Res* **44**, W90-97 (2016).
31. A, D. C. *et al.* Pattern of ascending aortic dimensions predicts the growth rate of the aorta in patients with bicuspid aortic valve. *JACC. Cardiovascular imaging* **6**, (2013).
32. Kalayinia, S., Arjmand, F., Maleki, M., Malakootian, M. & Singh, C. P. MicroRNAs: roles in cardiovascular development and disease. *Cardiovasc Pathol* **50**, 107296 (2021).
33. Lopez, A. *et al.* Predictors of Ascending Aorta Enlargement and Valvular Dysfunction Progression in Patients with Bicuspid Aortic Valve. *JCM* **10**, 5264 (2021).
34. Bissell, M. M. *et al.* Aortic dilation in bicuspid aortic valve disease: flow pattern is a major contributor and differs with valve fusion type. *Circ Cardiovasc Imaging* **6**, 499–507 (2013).
35. Meierhofer, C. *et al.* Wall shear stress and flow patterns in the ascending aorta in patients with bicuspid aortic valves differ significantly from tricuspid aortic valves: a prospective study. *Eur Heart J Cardiovasc Imaging* **14**, 797–804 (2013).

36. Guzzardi, D. G. *et al.* Valve-Related Hemodynamics Mediate Human Bicuspid Aortopathy: Insights From Wall Shear Stress Mapping. *Journal of the American College of Cardiology* **66**, 892–900 (2015).
37. Atkins, S. K. & Sucosky, P. Etiology of bicuspid aortic valve disease: Focus on hemodynamics. *World Journal of Cardiology* **6**, 1227–1233 (2014).
38. Andreassi, M. G. & Della Corte, A. Genetics of bicuspid aortic valve aortopathy. *Current Opinion in Cardiology* **31**, 585–592 (2016).
39. Drapisz, S., Góralczyk, T., Jamka-Miszalski, T., Olszowska, M. & Undas, A. Nonstenotic bicuspid aortic valve is associated with elevated plasma asymmetric dimethylarginine. *Journal of cardiovascular medicine (Hagerstown, Md.)* **14**, 446–52 (2013).
40. van de Pol, V. *et al.* Endothelial Colony Forming Cells as an Autologous Model to Study Endothelial Dysfunction in Patients with a Bicuspid Aortic Valve. *IJMS* **20**, 3251 (2019).
41. Ma, J., Sanchez-Duffhues, G., Goumans, M.-J. & ten Dijke, P. TGF-β-Induced Endothelial to Mesenchymal Transition in Disease and Tissue Engineering. *Frontiers in Cell and Developmental Biology* **8**, 260 (2020).
42. Maleki, S. *et al.* Endothelial/Epithelial Mesenchymal Transition in Ascending Aortas of Patients With Bicuspid Aortic Valve. *Front Cardiovasc Med* **6**, (2019).
43. Martínez-Micaelo, N. *et al.* Plasma Metabolomic Profiling Associates Bicuspid Aortic Valve Disease and Ascending Aortic Dilation with a Decrease in Antioxidant Capacity. *J Clin Med* **9**, (2020).
44. Alegret, J. M., Martínez-Micaelo, N., Aragonès, G. & Beltrán-Debón, R. Circulating endothelial microparticles are elevated in bicuspid aortic valve disease and related to aortic dilation. *International Journal of Cardiology* **217**, 35–41 (2016).
45. Cavallari, C. *et al.* miR-130a and Tgfβ Content in Extracellular Vesicles Derived from the Serum of Subjects at High Cardiovascular Risk Predicts their In-Vivo Angiogenic Potential. *Sci Rep* **10**, 706 (2020).
46. Moghaddam, A. S. *et al.* Cardioprotective microRNAs: Lessons from stem cell-derived exosomal microRNAs to treat cardiovascular disease. *Atherosclerosis* **285**, 1–9 (2019).
47. Dhahri, W. *et al.* Reduced expression of microRNA-130a promotes endothelial cell senescence and age-dependent impairment of neovascularization. *Aging (Albany NY)* **12**, 10180 (2020).
48. Singh, B. N. *et al.* Etv2-miR-130a-Jarid2 cascade regulates vascular patterning during embryogenesis. *PLoS One* **12**, e0189010 (2017).
49. Feng, Y. *et al.* MicroRNA-130a attenuates cardiac fibrosis after myocardial infarction through TGF-β/Smad signaling by directly targeting TGF-β receptor 1. *Bioengineered* **13**, 5779–5791.

Funding: This research was funded by a “Menudos Corazones” grant. BA-G received a research scholarship within the Martí-Franquès Research Fellowship Program from the University of Rovira i Virgili.

Institutional Review Board Statement: This study was conducted according to the principles of the Declaration of Helsinki and was approved by the Institutional Review Board and Ethics Committee (03-06-19/6proj4 and 114/2020) of our institutions, the Hospital Universitari Sant Joan and the Institut d’Investigació Sanitària Pere Virgili.

Informed Consent Statement: Informed consent was obtained from all subjects involved in the study.

Author’s Contributions: JM. A and R. CH conceptualized the experiments. B. AG wrote the original draft of the main manuscript, as well as figure preparation. JM. A and R. CH reviewed and edited the main manuscript for the final version. B. AG performed all the experiments, analysed the results and prepared the figures. R. CH was in charge of funding acquisition. N. MM: Helped in data curation and data analysis. J. supervised the methodology and results. C. MB, R. CH, B. C and JM. performed and reviewed the echocardiography. All authors reviewed the manuscript.

Conflicts of Interest: JM. A has a patent in miR-718 expression in aortic dilation in bicuspid aortic valve adults.

Figure Legend:

Figure 1. miRNA expression comparison between TAV, BAV_nonDIL and BAV_DIL patients. TAV: tricuspid aortic valve children; BAV_nonDIL: bicuspid aortic valve children without a dilated aorta; BAV_DIL: bicuspid aortic valve children with a dilated aorta. Data are presented as the mean ± SEM. Nonsignificant p values are not included in this figure.

Figure 2. Aortic dilation prediction with AUC graph in children.

Figure 3. Representation of the association between miR-130a dCt and aorta z scores in children**.** AA: Ascending aorta; AR: Aortic root.

Figure 4. Visualization of the strongest related miR-130a target gene predictions.

Figure 5. Related pathways to miR-130a gene targets.

Figure 6. Associated diseases to miR-130a gene targets.

Table 1. Clinical and echocardiographic characteristics:

				p. value			
	TAV	**BAV_nonDIL**	**BAV_DIL**	**Overall**	**TAV vs. BAV_nonDIL**	**TAV vs. BAV_DIL**	**BAV_nonDIL vs. BAV_DIL**
Age (years)	11.7 (3.0)	11.3 (3.9)	11.4 (3.8)	0.932	0.719	0.802	0.958
Sex (female)	13 (32.5%)	5.0 (20.8%)	6 (37.5%)	0.372	0.307	0.538	0.164
Weight (kg)	46.9 (16.4)	47.9 (22.0)	41.8 (15.8)	0.530	0.857	0.278	0.335
Height (cm)	153.4 (18.4)	149.8 (23.3)	147.3 (18.7)	0.546	0.494	0.264	0.725
BSA (m^2)	1.4 (0.3)	1.4 (0.4)	1.3 (0.3)	0.581	0.871	0.261	0.465
LVEDD (mm)	43.1 (4.9)	42.9 (5.5)	43.9 (6.0)	0.826	0.864	0.608	0.583
LVESD (mm)	28.3 (3.5)	27.4 (3.9)	28.5 (4.9)	0.610	0.388	0.799	0.406
EF (%)	63.8 (5.2)	65.6 (6.4)	64.0 (10.8)	0.593	0.221	0.937	0.563
Aortic root (mm)	22.75 (2.7)	24.5 (4.2)	26.7 (4.0)	**0.001**	0.086	**0.001**	0.113
Aortic root z score	-2.30 (0.8)	-0.8 (0.6)	1.9 (1.0)	**<0.001**	**<0.001**	**<0.001**	**<0.001**
Ascending aorta (mm)	20.8 (2.1)	23.9 (3.9)	30.1 (5.3)	**<0.001**	**0.001**	**<0.001**	**<0.001**
Ascending aorta z score	-0.2 (0.8)	1.2 (0.5)	3.6 (0.9)	**<0.001**	**<0.001**	**<0.001**	**<0.001**
AVG (mean; mmHg)	5.9 (0.6)	7.9 (4.4)	15.1 (9.8)	**<0.001**	**0.044**	**0.001**	**0.008**
AI (≥1)	0 (0.0%)	9 (37.5%)	12 (75%)	**<0.001**	**0.001**	**<0.001**	**0.013**
Typical BAV morphology (right-left)	-	12 (75%)	20 (83%)	-	-	-	**0.531**

TAV: tricuspid aortic valve children; BAV_nonDIL: bicuspid aortic valve children without a dilated aorta; BAV_DIL: bicuspid aortic valve children with a dilated aorta; BSA: body surface area; LVEDD: left ventricular end-diastolic diameter; LVESD: left ventricular end-systolic diameter; EF: ejection fraction; AVG: aortic valve gradient AI: aortic insufficiency

Data is represented as mean (SD).

Table 2. ANOVA between three groups:

				p. value			
	TAV	**BAV_non DIL**	**BAV_DIL**	**Overall**	**TAV vs. BAV_nonDIL p. value**	**TAV vs. BAV_DIL p. value**	**BAV_non DIL vs. BAV_DIL p. value**
miR-122 dCt	8.3 (1.5)	8.1 (1.5)	8.6 (1.5)	0.646	0.634	0.543	0.646
miR-130a dCt	5.5 (1.2)	5.8 (0.8)	6.5 (0.8)	**0.008**	0.326	**0.004**	**0.013**
miR-486 dCt	2.3 (1.7)	1.7 (2.3)	2.1 (2.0)	0.576	0.298	0.802	0.576
miR-718 dCt	11.4 (11.4)	11.3 (1.1)	11.0 (1.2)	0.478	0.589	0.249	0.478

TAV: tricuspid aortic valve children; BAV_nonDIL: bicuspid aortic valve children without a dilated aorta; BAV_DIL: bicuspid aortic valve children with a dilated aorta. Data is represented as ΔCt mean (SD).

Figure 1. miRNA expression comparison between TAV, BAV_nonDIL and BAV_DIL patients

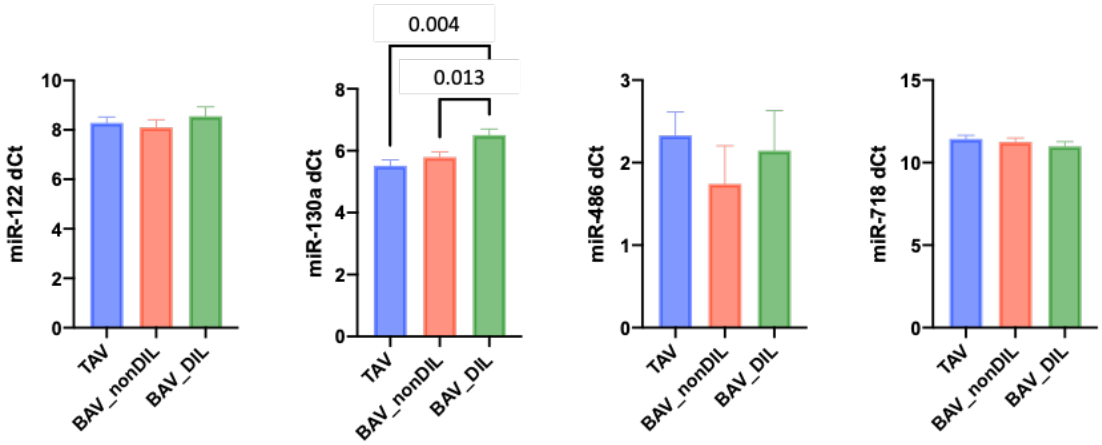

TAV: tricuspid aortic valve children; BAV_nonDIL: bicuspid aortic valve children without a dilated aorta; BAV_DIL: bicuspid aortic valve children with a dilated aorta. Data is represented as the ΔCt mean ± SEM. Nonsignificant p values are not included in this figure for clearer visualization.

Figure 2. Aortic dilation prediction with AUC graph in children:

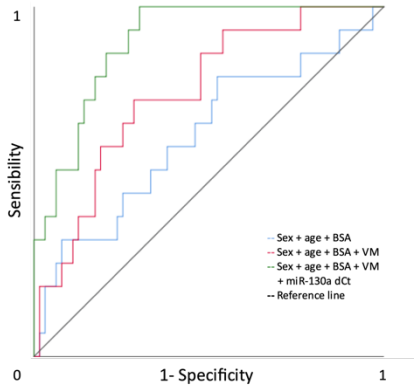

BSA: Body surface area; VM: Valve morphology

Table 3. Aortic dilation prediction models with AUC analysis:

	AUC	Error Dev.	p value	95% CI

Age + Sex + BSA	0.63	0.09	0.014	0.47-0.79
Age + Sex + BSA + VM	0.75	0.07	0.002	0.63-0.88
Age + Sex + BSA + VM + miR-130a dCt	0.90	0.04	<0.001	0.83-0.97

BSA: Body surface area; VM: Valve morphology

Table 4. Correlation analysis between microRNAs and aortic z scores

		AA z score	p value	AR z score	p value
TAV + BAV	**miR-122 dCt**	0.048	0.673	0.057	0.619
	miR-130a dCt	**0.318**	**0.004**	**0.322**	**0.004**
	miR-486 dCt	-0.054	0.633	-0.035	0.758
	miR-718 dCt	-0.103	0.361	-0.108	0.339
BAV	**miR-122 dCt**	0.136	0.402	0.137	0.404
	miR-130a dCt	**0.345**	**0.034**	**0.368**	**0.025**
	miR-486 dCt	0.017	0.914	0.019	0.905
	miR-718 dCt	-0.12	0.453	-0.122	0.455

AA: Ascending aorta; AR: Aortic root

Figure 3. Representation of the association between miR-130a dCt and aorta z scores in children

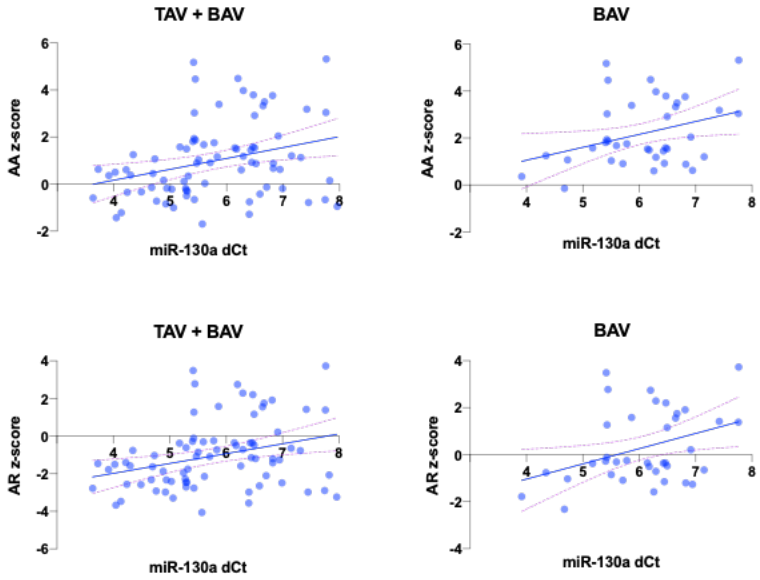

AA: Ascending aorta; AR: Aortic root

Table 5. Multivariate linear regression of parameters related to ascending aorta and aortic root z score

			B	Error Dev	ß	t	p. value
TAV+ BAV	**Ascending Aorta**	**Constant**	-1.693	0.968		-1.749	0.084
		miR-130[a] (by dCt)	0.464	0.164	0.308	2.822	**0.006**
	Aortic Root	**Constant**	-4.076	1.076		-3.790	**<0.001**
		miR-130a (by dCt)	0.524	0.182	0.315	2.870	**0.005**
BAV	**Ascending Aorta**	**Constant**	-1.141	1.528		-0.746	0.460
		miR-130a (by dCt)	0.549	0.249	0.345	2.207	**0.034**
	Aortic Root	**Constant**	-3.633	1.706		-2.130	**0.040**
		miR-130a (by dCt)	0.648	0.277	0.368	2.339	**0.025**

Figure 4. Visualization of the strongest related miR-130a target gene predictions:

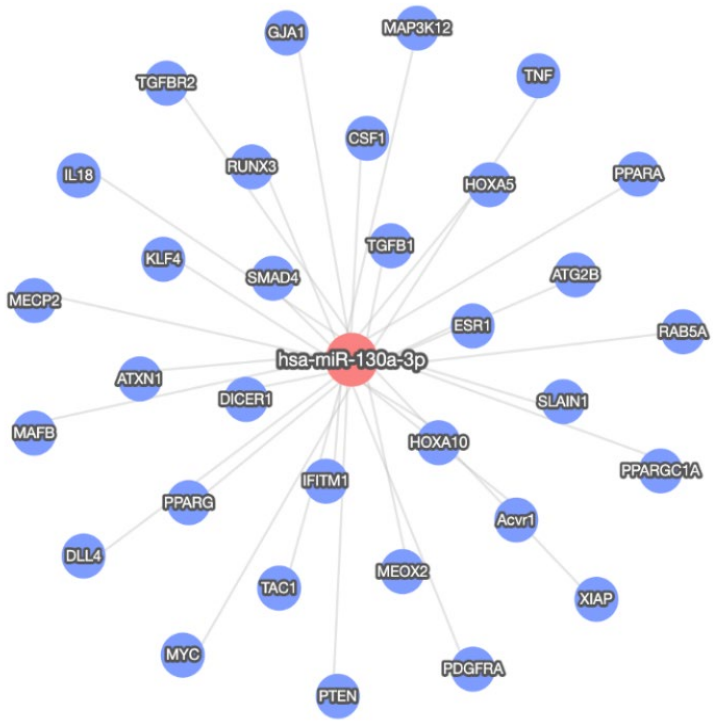

Figure 5. Related pathways to miR-130a gene targets:

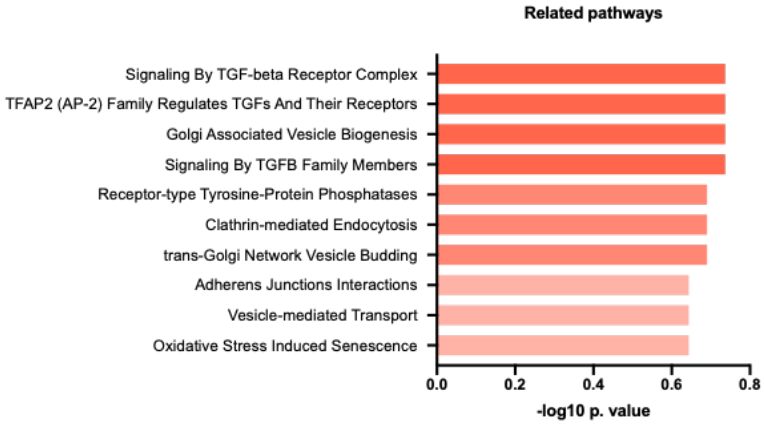

Figure 6. Associated diseases to miR-130a gene targets: